

Molecular structure and vibrational spectra of 1,3-bis(4-pyridyl)propane by quantum chemical calculations

Yusuf Erdoğdu, M. Tahir Güllüoğlu *, Mustafa Kurt

Ahi Evran Üniversitesi, Art and Science Faculty, Department of Physics, Aşıkpaşa Kampüsü, Kirşehir 40040, Turkey

Received 16 November 2007; received in revised form 31 December 2007; accepted 1 January 2008

Abstract

The experimental and theoretical study on the structures and vibrations of 1,3-bis(4-pyridyl)propane are presented. The FT-IR and Raman spectra of molecule have been measured. The optimized geometric bond lengths have been obtained by DFT show the best agreements with experimental values. The harmonic vibrational frequencies were calculated and scaled values have been compared with experimental FT-IR and FT-Raman spectra. Majority of the computed wavenumbers were found to be in good agreement with experimental observations. A complete assignment of the fundamentals was proposed based on the total energy distribution (TED) calculation.

© 2008 Elsevier B.V. All rights reserved.

Keywords: Density functional theory; 1,3-Bis(4-pyridyl)propane; Vibrational spectra

1. Introduction

Bpp is a very flexible versatile bifunctional ligand [1]. It is taken from aliphatic chain $-(\text{CH}_2)_3-$ between two pyridyl rings [2]. An extensive literature on network crystallized from different dipypyridyl ligand with various transition metal ions now exists. Networks prepared from flexible dipypyridyl ligands are of interest to many researchers because of the possible occurrence of different ligand conformations and consequently different topologies in polymeric structures can be reached by using this ligand [3,4]. Several workers determined crystal structures of transition metal and Bpp indicate the formation of polymeric structures with 1D, 2D and 3D network designs [3]. Bpp has been frequently used as a spacer for construction of polymeric compounds [5].

In our previous studies [6] we reported theoretical calculations of molecular structure and vibrational spectra of free 1,2-bis(4-pyridyl)ethane molecule. We are now reporting the results of calculation and experimental (IR and Raman) spectra of the Bpp molecule in HF and density functional theory (DFT) approximations. To the best of our knowledge, neither quantum chemical calculations nor the vibrational spectra of Bpp have been reported. Therefore, the present investigation was under-

taken to study the vibrational spectra of this molecule completely and to identify the various modes with greater wavenumber accuracy. Ab initio HF and density functional theory (DFT) calculations have been performed to support our wavenumber assignments.

2. Experimental

The 1,3-bis (4-pyridyl)propane samples were purchased from Sigma-Aldrich Chemical Company with a stated purity of greater than 98% and it was used as such without further purification. The sample of Bpp is in solid form at room temperature. The infrared spectrum of the sample was recorded between 4000 and 400 cm^{-1} on a Mattson 1000 FT-IR spectrometer which was calibrated using polystyrene bands. The sample was prepared as a KBr disc. The FT-Raman spectrum of the sample was recorded between 3500 and 5 cm^{-1} regions on a Bruker FRA 106/S FT-Raman instrument using 1064 nm excitation from an Nd:YAG laser. The detector is a liquid nitrogen cooled Ge detector.

3. Computational details

The molecular structure of Bpp (in vacuum) in the ground state is optimized by HF, BLYP and B3LYP with the 6-311G(d,p) and 6-31G(d) basis sets. Density functionals for all studies reported in this paper have the fol-

* Corresponding author. Tel.: +90 386 252 80 50; fax: +90 386 252 80 54.

E-mail address: mtahir@gazi.edu.tr (M. Tahir Güllüoğlu).

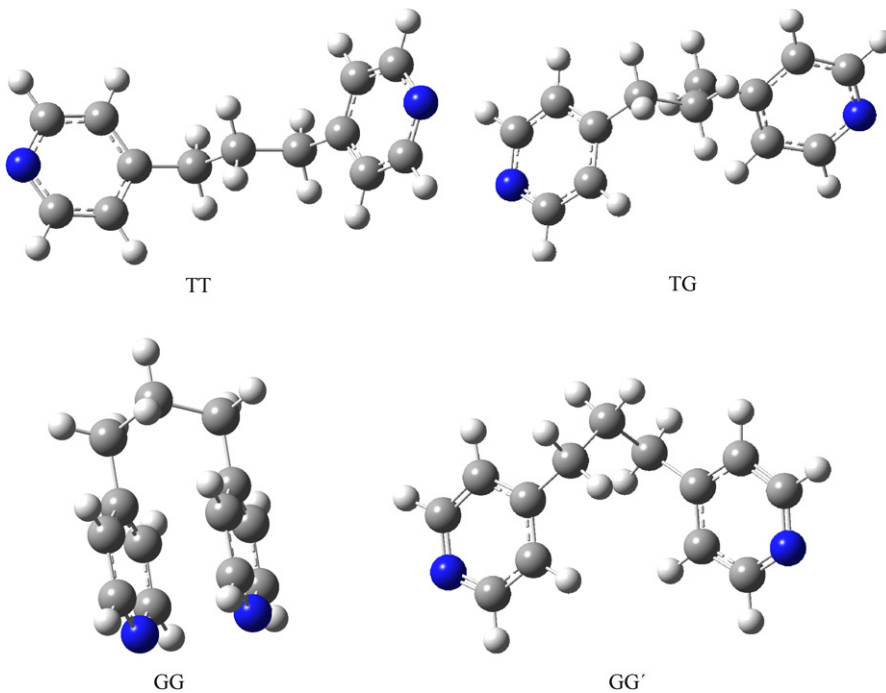


Fig. 1. Kinds of Bpp ligand conformation.

lowing form: $E_{\text{XC}} = (1 - a_0)E_{\text{X}}^{\text{LSDA}} + a_0E_{\text{X}}^{\text{HF}} + a_X\Delta E_{\text{X}}^{\text{B88}} + a_cE_{\text{C}}^{\text{LYP}} + (1 - a_c)E_{\text{C}}^{\text{VWN}}$ where the energy terms are the Slater exchange, the Hartree–Fock exchange, Becke's exchange functional correction, and the gradient corrected correlation functional of Lee, Yang and Parr and the local correlation functional of Vosko et al. [7]. RHF, RB3LYP, RBLYP with 6-311G(d,p) and 6-31G(d) levels of theory with the optimized geometries have been used to calculate all parameters of Bpp molecule.

Three sets of vibrational frequencies for these species are calculated with these methods and then scaled by corresponding scaling factors [8]. All the calculations are performed by using Gauss-view molecular visualization program and Gaussian 03 program package on the personal computer [9,10]. These calculations are valuable to take insight into the vibrational spectroscopy and molecular parameters of structure.

4. Results and discussion

4.1. Geometrical structures

This is the fist report on molecular structure and vibrational spectra of Bpp molecule by using DFT and HF methods. From Fig. 1, it can be seen that the structures of Bpp molecule can adopt four discrete conformations. These conformations are *Transoid–Transoid* (TT), *Transoid–Gauche* (TG), *Gauche–Gauche* (GG) and *Gauche–Gauche* (GG') [11,12]. Bpp ligand adopts a *Transoid–Transoid* conformation with dihedral angles of -180° ($\text{C}_3-\text{C}_{11}-\text{C}_{14}-\text{C}_{17}$) and 180° ($\text{C}_{11}-\text{C}_{14}-\text{C}_{17}-\text{C}_{20}$). The molecule of Bpp is the most stable in TT conformation. Therefore structure of Bpp has been optimized at the DFT and HF levels of theory using 6-31G(d) and 6-311G(d,p) basis sets. The symmetry of different conformations

Table 1

The selected molecular properties of conformation of the Bpp (with the B3LYP/6-311G(d,p)/6-31G(d))

	TT	TG	GG	GG'
Symmetry	C_{2v}	C_1	C_s	C_2
Energy (a.u.)	$-613.467461377,$ -613.318781773	$-613.466949370,$ -613.318372859	$-613.461399530,$ -613.313177835	$-613.465974102,$ -613.317657765
Energy diff. (kcal/mol)	0.0, 0.0	0.321, 0.256	3.803, 3.516	0.933, 0.705
E_{HOMO}	$-0.591, -0.277$	$-0.0564, -0.244$	$-0.273, -0.292$	$-0.536, -0.225$
E_{LUMO}	0.771, 2.114	0.897, 2.260	0.813, 2.140	0.876, 2.237
$\Delta E_{\text{HOMO-LUMO}}$ (eV)	1.362, 2.391	1.461, 2.504	1.086, 2.432	1.412, 2.462
N–N distances (Å)	9.709, 9.710 [9.1–10.1] ^a	8.997, 9.007 [8.6–9.2] ^a	5.111, 5.053 [3.9] ^a	8.134, 8.504 [6.7–8.6] ^a
Dipole moment (Debye)	2.7156, 2.7259	2.7508, 2.7358	4.7970, 4.7913	2.9050, 2.9374
$\text{C}_3-\text{C}_{11}-\text{C}_{14}-\text{C}_{17}$	180.0, 180.0	65.81, 65.501	75.96, 75.50	64.92, 63.919
$\text{C}_{11}-\text{C}_{14}-\text{C}_{17}-\text{C}_{20}$	$-180.0, -180.0$	$-179.75, 179.966$	$-75.96, -75.50$	$-64.92, -63.919$

^a Taken from Ref. [11].

Table 2

Bond lengths and bond angles for Bpp (TT Conformation)

	B3LYP			BLYP			HF			Exp. [6]	Exp. [13]
	6-311G(d,p)		Bpp	6-311G(d,p)		Bpp	6-311G(d,p)		Bpp		
	Bpp	Bpp	Bpe [6]	Bpp	Bpp	Bpe [6]	Bpp	Bpp	Bpe [6]		
Bond lengths (Å)											
C ₁ –C ₂	1.392	1.394	1.394	1.401	1.404	1.404	1.383	1.383	1.384	1.383	1.380
C ₁ –N ₆	1.336	1.339	1.338	1.349	1.352	1.352	1.319	1.320	1.320	1.323	1.338
C ₁ –H ₇	1.086	1.089		1.0936	1.096		1.076	1.076			0.93
C ₂ –C ₃	1.397	1.399	1.399	1.407	1.410	1.410	1.387	1.388	1.388	1.373	1.391
C ₂ –H ₈	1.085	1.087		1.092	1.095		1.075	1.075			0.93
C ₃ –C ₄	1.397	1.399	1.399	1.407	1.410	1.410	1.387	1.388	1.388	1.382	1.386
C ₃ –C ₁₁	1.509	1.511	1.511	1.519	1.521	1.520	1.510	1.511	1.511	1.509	1.501
C ₄ –C ₅	1.392	1.394	1.394	1.401	1.404	1.404	1.383	1.383	1.384	1.364	1.374
C ₄ –H ₉	1.085	1.087		1.092	1.095		1.075	1.075			0.93
C ₅ –N ₆	1.336	1.339	1.338	1.349	1.352	1.352	1.319	1.320	1.320	1.323	1.338
C ₅ –H ₁₀	1.086	1.089		1.093	1.096		1.076	1.076			0.93
C ₁₁ –H ₁₂	1.095	1.097		1.101	1.105		1.086	1.086			0.97
C ₁₁ –H ₁₃	1.095	1.097		1.101	1.105		1.086	1.086			0.97
C ₁₁ –C ₁₄	1.541	1.542	1.552	1.554	1.555	1.566	1.535	1.535	1.542	1.498	1.525
C ₁₄ –H ₁₅	1.094	1.097		1.101	1.104		1.086	1.086			0.97
C ₁₄ –H ₁₆	1.094	1.097		1.101	1.104		1.086	1.086			0.97
C ₁₄ –C ₁₇	1.541	1.542		1.554	1.555		1.535	1.535		1.498	1.525
C ₁₇ –H ₁₈	1.095	1.097		1.101	1.105		1.086	1.086			0.97
C ₁₇ –H ₁₈	1.095	1.097		1.101	1.105		1.086	1.086			0.97
C ₁₇ –C ₂₀	1.509	1.511	1.511	1.519	1.521	1.520	1.510	1.511	1.511	1.498	1.501
C ₂₀ –C ₂₁	1.397	1.399	1.399	1.407	1.410	1.410	1.387	1.388	1.388	1.373	1.391
C ₂₀ –C ₂₂	1.397	1.399	1.399	1.407	1.410	1.410	1.387	1.388	1.388	1.382	1.386
C ₂₁ –C ₂₃	1.392	1.394	1.394	1.401	1.404	1.404	1.383	1.383	1.384	1.383	1.380
C ₂₁ –H ₂₄	1.085	1.087		1.092	1.095		1.075	1.075			0.93
C ₂₂ –C ₂₅	1.392	1.394	1.394	1.401	1.404	1.404	1.383	1.383	1.384	1.364	1.374
C ₂₂ –H ₂₆	1.085	1.087		1.092	1.095		1.075	1.075			0.93
C ₂₃ –N ₂₇	1.336	1.339	1.338	1.349	1.352	1.352	1.319	1.320	1.320	1.323	1.374
C ₂₃ –H ₂₈	1.086	1.089		1.093	1.096		1.076	1.076			0.93
C ₂₅ –N ₂₇	1.336	1.339	1.338	1.349	1.352	1.352	1.319	1.320	1.320		1.374
C ₂₅ –H ₂₉	1.086	1.089		1.093	1.096		1.076	1.076			0.93
Bond angles (°)											
C ₂ –C ₁ –N ₆	123.8	123.9	123.8	123.9	124.0	124.0	123.8	123.7	123.6	124.5	123.1
C ₂ –C ₁ –H ₇	120.1	120.0		120.1	120.0		120.0	120.0			118.4
N ₆ –C ₁ –H ₇	116.0	116.0		115.8	115.8		116.1	116.1			118.4
C ₁ –C ₂ –C ₃	119.4	119.4	119.4	119.5	119.4	119.4	119.1	119.2	119.1	119.2	119.5
C ₁ –C ₂ –H ₈	119.8	119.9		119.8	119.4		119.8	119.8			120.0
C ₃ –C ₂ –H ₈	120.6	120.6		120.6	120.5		120.9	120.9			120.0
C ₂ –C ₃ –C ₄	116.7	116.7	116.8	116.7	116.7	116.7	116.8	116.9	116.9	116.7	116.7
C ₂ –C ₃ –C ₁₁	121.6	121.6	121.5	121.6	121.6	121.6	121.5	121.5	121.5	121.0	122.5
C ₄ –C ₃ –C ₁₁	121.6	121.6		121.6	121.6		121.5	121.5			122.6
C ₃ –C ₄ –C ₅	119.4	119.4	119.4	119.5	119.4	119.4	119.1	119.2	119.1	119.3	120.3
C ₃ –C ₄ –H ₉	120.6	120.6		120.6	120.5		120.9	120.9			119.8
C ₅ –C ₄ –H ₉	119.8	119.9		119.8	119.9		119.8	119.8			119.8
C ₄ –C ₅ –N ₆	123.8	123.9	123.8	123.9	124.0	124.0	123.8	123.7	123.8	125.0	122.7
C ₄ –C ₅ –H ₁₀	120.1	120.0		120.1	120.0		120.0	120.0			118.6
N ₆ –C ₅ –H ₁₀	116.0	116.0		115.8	115.8		116.1	116.1			118.6
C ₁ –N ₆ –C ₅	116.6	116.5	116.5	116.3	116.1	116.2	117.1	117.1	117.1	115.3	117.3
C ₃ –C ₁₁ –H ₁₂	109.4	109.6		109.4	109.6		109.2	109.3			109.3
C ₃ –C ₁₁ –H ₁₃	109.4	109.6		109.4	109.6		109.2	109.3			109.3
C ₃ –C ₁₁ –C ₁₄	112.6	112.5	112.2	112.8	112.6	112.4	112.5	112.4	112.0	112.6	111.5
H ₁₂ –C ₁₁ –H ₁₃	106.7	106.6		106.7	106.7		106.8	106.7			108.0
H ₁₂ –C ₁₁ –C ₁₄	109.1	109.0		109.0	108.9		109.4	109.3			109.3
H ₁₃ –C ₁₁ –C ₁₄	109.1	109.0		109.0	108.9		109.4	109.3			109.3
C ₁₁ –C ₁₄ –H ₁₅	109.4	109.5		109.4	109.4		109.5	109.5			109.3
C ₁₁ –C ₁₄ –H ₁₆	109.4	109.5		109.4	109.4		109.5	109.5			109.3
C ₁₁ –C ₁₄ –C ₁₇	112.4	112.4	112.2	112.5	112.5	112.4	112.2	112.1	112.0	112.6	111.7
H ₁₅ –C ₁₄ –H ₁₆	106.2	106.1		106.2	106.2		106.4	106.4			107.9
H ₁₅ –C ₁₄ –C ₁₇	109.4	109.5		109.4	109.4		109.5	109.5			109.3

Table 2 (Continued)

	B3LYP		BLYP			HF		Exp. [6]	Exp. [13]
	6-311G(d,p)		6-311G(d,p)		6-311G(d,p)		6-311G(d,p)		
	Bpp	Bpp	Bpe [6]	Bpp	Bpp	Bpe [6]	Bpp	Bpp	Bpe [6]
H ₁₆ –C ₁₄ –C ₁₇	109.4	109.5		109.4	109.4		109.5	109.5	109.3
C ₁₄ –C ₁₇ –H ₁₈	109.1	109.0		109.0	108.9		109.4	109.3	109.3
C ₁₄ –C ₁₇ –H ₁₉	109.1	109.0		109.0	108.9		109.4	109.3	109.3
C ₁₄ –C ₁₇ –C ₂₀	112.6	112.5	112.0	112.8	112.6	112.0	112.5	112.4	112.0
H ₁₈ –C ₁₇ –H ₁₉	106.7	106.6		106.7	106.7		106.8	106.7	108.8
H ₁₈ –C ₁₇ –C ₂₀	109.4	109.6		109.4	109.6		109.2	109.3	109.3
H ₁₉ –C ₁₇ –C ₂₀	109.4	109.6		109.4	109.6		109.2	109.3	109.3
C ₁₇ –C ₂₀ –C ₂₁	121.6	121.60	119.4	121.6	121.6	119.4	121.5	121.5	119.1
C ₁₇ –C ₂₀ –C ₂₂	121.6	121.6	119.4	121.6	121.6	119.4	121.5	121.5	119.1
C ₂₁ –C ₂₀ –C ₂₂	116.7	116.7	116.8	116.7	116.7	116.7	116.8	116.9	116.7
C ₂₀ –C ₂₁ –C ₂₃	119.4	119.4	119.4	119.5	119.4	119.4	119.1	116.9	119.1
C ₂₀ –C ₂₁ –H ₂₄	120.6	120.6		120.6	120.5		120.9	120.9	120.2
C ₂₃ –C ₂₁ –H ₂₄	119.8	119.9		119.8	119.9		119.8	119.8	120.2
C ₂₀ –C ₂₂ –C ₂₅	119.4	119.4	119.4	119.5	119.4	119.4	119.1	119.2	120.3
C ₂₀ –C ₂₂ –H ₂₆	120.6	120.6		120.6	120.5		120.9	120.9	119.8
C ₂₅ –C ₂₂ –H ₂₆	119.8	119.9		119.8	119.9		119.8	119.8	119.8
C ₂₁ –C ₂₃ –N ₂₇	123.8	123.9	123.8	123.9	124.0	124.0	123.8	123.7	123.6
C ₂₁ –C ₂₃ –H ₂₈	120.1	120.0		120.1	120.0		120.0	120.0	118.4
N ₂₇ –C ₂₃ –H ₂₈	116.0	116.0		115.8	115.8		116.1	116.1	118.4
C ₂₂ –C ₂₅ –N ₂₇	123.8	123.9	123.8	123.9	124.0	124.0	123.8	123.7	123.8
C ₂₂ –C ₂₅ –H ₂₉	120.1	120.0		120.1	120.0		120.0	120.0	118.6
N ₂₇ –C ₂₅ –H ₂₉	116.0	116.0		115.8	115.8		116.1	116.1	118.6
C ₂₃ –N ₂₇ –C ₂₅	116.6	116.5	116.5	116.3	116.1	116.2	117.1	117.1	115.3
									117.3

of Bpp has the C_{2v} (TT), C_1 (TG), C_s (GG) and C_2 (GG'). The calculation of the harmonic vibrational frequencies, IR intensities and Raman scattering activities were performed on the basis of the optimized structure. The main optimized molecular parameters were presented in Table 1 and Table 2. The labeling of atoms in Bpp is given in Fig. 2. Optimized geometric parameters of Bpp compared with those of Zn(Bpp)Cl₂ [13] and 1,2-bis(4-pyridyl)ethane [6].

4.2. Assignment of fundamentals

In TT conformation of Bpp belongs to C_{2v} symmetry and it has 29 atoms. This conformation has minimum energy profile. The 81 normal vibrations are distributed as $23A_1 + 18A_2 + 19B_1 + 21B_2$. The fundamentals of A_1 and B_1 symmetry correspond to in-plane normal modes and those of B_2 and A_2 to out of plane normal modes. All fundamentals are

Raman active but only the vibrations of A_1 , B_1 and B_2 symmetry will be present in the IR spectrum. The observed and calculated wavenumber of the Bpp molecule are given in Table 3. The total energy distribution (TED) was calculated by using the Parallel Quantum Solutions program [14] and fundamental vibrational modes were characterized by their TED.

Figs. 3 and 4 present the FT-Raman and FT-IR spectra of Bpp, respectively. The calculated IR spectra are shown in Fig. 5 for comparative purposes. The experimental FT-IR and FT-Raman wavenumbers are tabulated in Table 3 together with the calculated wavenumbers. For better identification of main frequencies of Bpp, the assignment of the fundamentals and the result of the

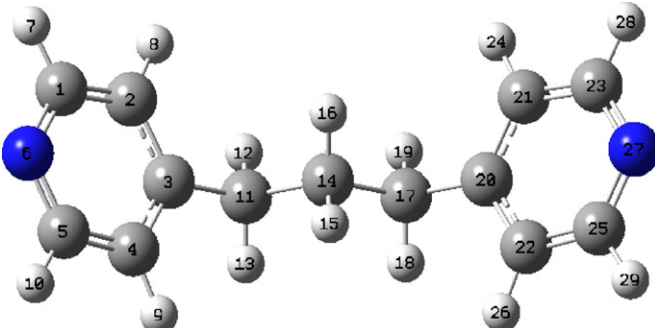


Fig. 2. Bpp structure and atoms numbering (TT conformation).

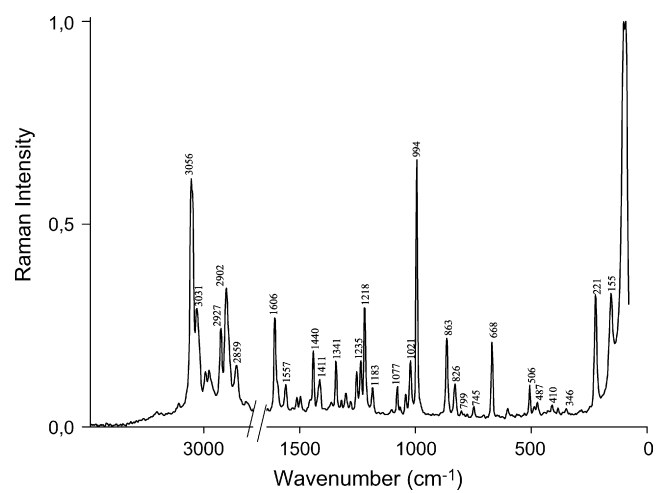


Fig. 3. The Raman spectra of Bpp.

Table 3

Comparison of the observed and calculated vibrational spectra of free Bpp (TT conformation)

Mode	HF		B3LYP						BLYP		Bpp		Bpe [6]		TED ^g (%)		
	6-311G(d,p)		6-31G(d)		6-311G(d,p)		6-31G(d)		6-311G(d,p)		6-31G(d)		Exp. IR	Exp. RA			
	Bpp		Bpp		Bpp		Bpp		Bpp		Bpp		Exp IR/RA	Mode			
	Freq. ^a	Freq. ^b	Freq. ^c	IR	RA	Freq. ^d	IR	RA	Freq.	Freq. ^e	Freq.	Freq. ^f					
<i>v</i> ₁	<i>A</i> ₂	18	17	8	0.000	6.403	11	0.000	7.493	24	4	11			$\Gamma_{\text{HCC}}(44) + \Gamma_{\text{CCCC}}(42)$ (P-ME)		
<i>v</i> ₂	<i>B</i> ₁	24	23	17	0.671	7.295	16	0.638	8.384	37	15	16			$\Gamma_{\text{CCCC}}(67)$ (M)		
<i>v</i> ₃	<i>A</i> ₁	42	41	39	0.957	6.600	39	1.013	7.374	54	39	39			$\delta_{\text{CCC}}(33)$ (P-M) + $\Gamma_{\text{CCCC}}(17)$ (P-M) + $\delta_{\text{CCC}}(11)$ (M)		
<i>v</i> ₄	<i>A</i> ₂	67	67	69	0.000	0.711	69	0.000	0.572	58	70	71			$\Gamma_{\text{CCCC}}(35)$ (P-M) + $\Gamma_{\text{HCC}}(30)$ + $\Gamma_{\text{HCC}}(14)$ + $\delta_{\text{CCC}}(12)$		
<i>v</i> ₅	<i>B</i> ₁	100	98	105	0.045	0.105	105	0.067	0.038	107	108		99	vs	$\Gamma_{\text{HCC}}(75) + \Gamma_{\text{CCCC}}(25)$		
<i>v</i> ₆	<i>B</i> ₂	116	115	111	0.532	0.630	110	0.761	0.863	114	109	110			$\Gamma_{\text{CCCC}}(36) + \delta_{\text{CCC}}(16)$ + $\Gamma_{\text{HCC}}(14)$		
<i>v</i> ₇	<i>A</i> ₁	213	212	211	1.053	2.880	210	1.104	3.084	209	210				$\delta_{\text{CCC}}(19) + v_{\text{C}-\text{CH}_2}(17) + v_{\text{CC}}(16)$		
<i>v</i> ₈	<i>A</i> ₁	237	236	233	0.047	0.959	232	0.121	1.186	226	231	232		221	m	$\delta_{\text{CCC}}(25) + \Gamma_{\text{CCCC}}(20)$ (M)	
<i>v</i> ₉	<i>B</i> ₂	330	327	329	0.277	0.206	326	0.290	0.068	282	327	327			$\delta_{\text{CCC}}(26) + \Gamma_{\text{CCCC}}(18)$ (M)		
<i>v</i> ₁₀	<i>B</i> ₁	336	334	329	0.205	0.130	327	0.060	0.219	303	331	328			$\delta_{\text{CCC}}(79)$		
<i>v</i> ₁₁	<i>A</i> ₂	337	334	336	0.000	0.069	334	0.000	0.087	357	338	337			$\delta_{\text{CCC}}(70)$		
<i>v</i> ₁₂	<i>A</i> ₂	399	396	375	0.000	0.002	374	0.000	0.003	375	366	367			$\Gamma_{\text{CCCN}}(40) + \Gamma_{\text{HCC}}(16) + \Gamma_{\text{HCCN}}(13)$		
<i>v</i> ₁₃	<i>B</i> ₁	399	396	375	0.001	0.018	374	0.000	0.094	376	366	368	403	vw	$\Gamma_{\text{CCCN}}(40) + \Gamma_{\text{HCC}}(16) + \Gamma_{\text{HCCN}}(13)$		
<i>v</i> ₁₄	<i>B</i> ₂	499	494	495	20.986	3.157	491	18.414	3.375	480	495	493	485	s	487	vw	$\delta_{\text{CCC}}(16) + v_{\text{C}-\text{CH}_2}(14) + \delta_{\text{CNC}}(9)$
<i>v</i> ₁₅	<i>A</i> ₁	519	515	507	18.051	1.921	504	11.615	1.697	504	505	504	505	s	506	w	$\Gamma_{\text{CNCC}}(19) + \Gamma_{\text{CNCH}}(14) + \Gamma_{\text{CCCC}}(13)$
<i>v</i> ₁₆	<i>B</i> ₂	588	583	578	4.2082	0.060	574	2.961	0.076	541	577	575	577	m	547	vs (547 vs)	$\delta_{\text{CCC}}(36) + \Gamma_{\text{CNCC}}(14) + \Gamma_{\text{CNCH}}(13)$
<i>v</i> ₁₇	<i>A</i> ₁	593	587	588	16.599	2.536	582	14.970	2.481	604	588	584	603	s			$\delta_{\text{NCC}}(16) + \delta_{\text{CCC}}(14)$ (PY) + $v_{\text{CC}}(8)$ + $\delta_{\text{CCC}}(4)$ (M)
<i>v</i> ₁₈	<i>A</i> ₂	667	663	663	0.000	8.195	659	0.000	8.534	660	664	662	670	vw	668	m	$\delta_{\text{NCC}}(31) + \delta_{\text{CCC}}(26)$
<i>v</i> ₁₉	<i>B</i> ₁	667	663	663	0.659	3.441	660	0.804	3.548	661	664	662				$\delta_{\text{NCC}}(31) + \delta_{\text{CCC}}(26)$	
<i>v</i> ₂₀	<i>B</i> ₁	721	717	720	0.857	0.004	722	0.651	0.044	729	725	727				$\Gamma_{\text{HCC}}(64)$	
<i>v</i> ₂₁	<i>A</i> ₁	747	739	737	0.046	2.287	729	0.594	3.067	736	734	730				$\Gamma_{\text{CNCC}}(23) + \Gamma_{\text{HCC}}(16) + \Gamma_{\text{CCCC}}(12) + \Gamma_{\text{CCCN}}(10)$	
<i>v</i> ₂₂	<i>B</i> ₂	754	747	742	0.083	0.050	735	0.704	0.053	754	739	733				$\Gamma_{\text{CNCC}}(23) + \Gamma_{\text{CCCN}}(19) + \Gamma_{\text{CCCC}}(14)$	
<i>v</i> ₂₃	<i>B</i> ₂	785	780	781	31.558	0.386	777	26.448	0.591	782	778	776	743	w	745	vw	$v_{\text{C}-\text{CH}_2}(26) + v_{\text{CC}}(15) + v_{\text{CC}}(11)$
<i>v</i> ₂₄	<i>A</i> ₁	816	811	793	32.250	12.251	789	21.766	11.153	787	787	786				$\Gamma_{\text{HCCN}}(23) + \Gamma_{\text{CCCC}}(20) + \Gamma_{\text{CCCN}}(18)$ (M)	
<i>v</i> ₂₅	<i>B</i> ₂	828	826	821	5.552	0.009	815	3.108	0.005	807	814	812	784	vs	799	vw	$\Gamma_{\text{CCCC}}(22) + \Gamma_{\text{CCCC}}(21)$ (M)
<i>v</i> ₂₆	<i>A</i> ₂	843	838	822	0.000	0.425	824	0.000	0.924	824	826	830				$\Gamma_{\text{CCCC}}(25) + \delta_{\text{CCH}}(16)$	
<i>v</i> ₂₇	<i>A</i> ₁	847	841	836	10.574	9.853	833	8.504	9.070	858	832	831	831	s	826	w	$v_{\text{C}-\text{CH}_2}(23) + v_{\text{CC}}(23) + v_{\text{CC}}(11)$ (M) + $\delta_{\text{CNC}}(11)$
<i>v</i> ₂₈	<i>B</i> ₁	884	879	859	0.012	1.346	855	0.016	6.510	858	854	854	855	s	863	m	$\Gamma_{\text{CCCC}}(63) + \Gamma_{\text{NCCN}}(24)$
<i>v</i> ₂₉	<i>A</i> ₂	885	879	860	0.000	0.187	855	0.000	2.299	859	855	854				$\Gamma_{\text{CCCC}}(63) + \Gamma_{\text{NCCN}}(24)$	
<i>v</i> ₃₀	<i>A</i> ₁	989	982	949	0.099	2.180	938	0.325	2.083	940	938	930				$\Gamma_{\text{HCC}}(50) + \Gamma_{\text{CCCC}}(14)$	
<i>v</i> ₃₁	<i>B</i> ₂	989	982	951	0.069	0.070	939	0.173	0.559	942	940	931				$\Gamma_{\text{HCC}}(51) + \Gamma_{\text{CCCC}}(12)$	
<i>v</i> ₃₂	<i>A</i> ₂	990	983	970	0.000	0.326	952	0.000	0.915	955	955	939				$\Gamma_{\text{HCC}}(46) + \Gamma_{\text{CNCH}}(23) + \Gamma_{\text{CCCC}}(14)$	
<i>v</i> ₃₃	<i>B</i> ₁	991	984	970	0.007	0.413	952	0.007	1.602	955	955	939				$\Gamma_{\text{HCC}}(47) + \Gamma_{\text{CNCH}}(23) + \Gamma_{\text{CCCC}}(14)$	
<i>v</i> ₃₄	<i>B</i> ₂	999	994	978	6.067	12.218	972	5.452	11.144	974	970	967	991	s	994	s	$v_{\text{CN}}(26) + v_{\text{CC}}(16) + \delta_{\text{CCC}}(6) + \delta_{\text{NCC}}(6)$
<i>v</i> ₃₅	<i>A</i> ₁	1008	1011	978	4.113	52.781	972	3.615	44.337	975	971	968				$v_{\text{CN}}(26) + v_{\text{CC}}(16) + \delta_{\text{CCC}}(7) + \delta_{\text{NCC}}(7)$	
<i>v</i> ₃₆	<i>B</i> ₂	1023	1013	991	6.006	1.630	992	5.641	4.021	976	975	979				$v_{\text{CC}}(89)$	
<i>v</i> ₃₇	<i>A</i> ₁	1023	1013	1003	0.485	64.550	1003	0.465	67.341	980	990	993				$v_{\text{CC}}(55) + \delta_{\text{CCC}}(23)$	
<i>v</i> ₃₈	<i>B</i> ₁	1024	1018	1007	0.003	0.004	1012	0.094	0.266		1007	1015	1021	w	1021	w	$\Gamma_{\text{HCC}}(26) + \delta_{\text{CCH}}(19) + \Gamma_{\text{HCC}}(18) + v_{\text{cc}}(13)$
<i>v</i> ₃₉	<i>B</i> ₂	1046	1055	1056	3.188	1.539	1056	2.216	1.847	1058	1054	1056	1038	w	1039	vw	$\delta_{\text{CCH}}(30) + v_{\text{CN}}(22)$
<i>v</i> ₄₀	<i>A</i> ₁	1058	1062	1056	0.641	3.243	1056	0.356	3.449	1059	1054	1056				$\delta_{\text{CCH}}(30) + v_{\text{CN}}(22)$	
<i>v</i> ₄₁	<i>A</i> ₂	1066	1063	1061	0.000	0.386	1063	0.000	0.529	1068	1059	1063	1065	w	1077	w	$v_{\text{CC}}(26) + \delta_{\text{CCH}}(18)$
<i>v</i> ₄₂	<i>B</i> ₁	1066	1064	1080	0.064	0.011	1083	0.228	0.033	1083	1081	1087	1092	w			$v_{\text{CC}}(30) + \delta_{\text{CCH}}(25)$
<i>v</i> ₄₃	<i>A</i> ₂	1073	1073	1108	0.000	0.347	1112	0.000	1.437	1129	1115	1121				$\delta_{\text{CCH}}(33)$	
<i>v</i> ₄₄	<i>B</i> ₂	1141	1145	1190	0.355	2.290	1190	0.974	1.4050	1196	1185	1189				$v_{\text{C}-\text{CH}_2}(30) + \delta_{\text{CCH}}(15) + v_{\text{CC}}(13)$	
<i>v</i> ₄₅	<i>A</i> ₁	1173	1175	1194	0.002	45.104	1195	0.008	41.445	1196	1190	1194				$v_{\text{C}-\text{CH}_2}(29) + \delta_{\text{CCH}}(18) + v_{\text{CC}}(13)$	

Table 3 (Continued)

Mode	HF		B3LYP						BLYP		Bpe [6]			TED ^g (%)	
	6-31G(d,p)		6-31G(d)		6-31G(d,p)		6-31G(d)		6-31G(d,p)		Exp. IR	Exp. RA	Exp IR/RA		
	Bpp	Bpp	Bpp	IR	RA	Bpp	IR	RA	Bpp	Bpp				Mode	
	Freq. ^a	Freq. ^b	Freq. ^c			Freq. ^d			Freq.	Freq. ^e					
v_{46}	B_2	1198	1194	1204	7.165	2.071	1207	4.835	2.429	1210	1203	1210		$\delta_{\text{NCH}}(29) + \nu_{\text{CN}}(18) + \delta_{\text{CCH}}(18) + \nu_{\text{CC}}(15)$	
v_{47}	A_1	1203	1199	1205	4.703	10.253	1208	3.795	12.319	1210	1204	1210	1215 m	1218 s	$\delta_{\text{NCH}}(21) + \delta_{\text{CCH}}(20) + \nu_{\text{CC}}(19) + \nu_{\text{CN}}(17)$
v_{48}	B_1	1216	1215	1218	0.680	0.151	1230	1.014	0.459	1245	1222	1238	1227 m		$\nu_{\text{CN}}(25) + \nu_{\text{CC}}(22) + \delta_{\text{CCH}}(17)$
v_{49}	B_2	1216	1215	1230	0.716	2.168	1233	0.031	3.077	1261	1233	1238			$\delta_{\text{CCH}}(35) + \Gamma_{\text{HCCH}}(15) + \nu_{\text{CC}}(13)$
v_{50}	A_2	1250	1250	1243	0.000	11.046	1259	0.000	9.991	1245	1266	1266			$\nu_{\text{CN}}(48) + \nu_{\text{CC}}(36)$
v_{51}	B_1	1265	1265	1262	0.004	1.366	1273	0.015	0.984	1266	1265	1279	1252 vw	1253 w	$\delta_{\text{CCH}}(34) + \nu_{\text{CN}}(27) + \nu_{\text{CC}}(13)$
v_{52}	A_2	1302	1300	1283	0.000	15.231	1287	0.000	26.363	1280	1286	1293			$\delta_{\text{CCH}}(62)$
v_{53}	A_1	1343	1342	1311	2.328	49.634	1318	2.483	51.329	1308	1319	1302 vw	1299 vw	1300 w	$\delta_{\text{CCH}}(48) + \Gamma_{\text{CCCH}}(13) + \nu_{\text{CC}}(7)$
v_{54}	A_2	1344	1343	1322	0.000	0.027	1327	0.000	0.019	1329	1325	1333			$\delta_{\text{CCH}}(55) + \delta_{\text{NCH}}(19)$
v_{55}	B_1	1344	1345	1324	0.444	0.913	1328	0.794	1.450	1332	1326	1335	1318 vw	1318 vw	$\delta_{\text{CCH}}(58) + \delta_{\text{NCH}}(19)$
v_{56}	B_2	1388	1390	1335	1.943	3.905	1346	1.404	10.133	1337	1326	1341	1340 m	1341 m	$\delta_{\text{CCH}}(43) + \Gamma_{\text{HCCH}}(19)$
v_{57}	A_2	1418	1417	1398	0.000	1.558	1403	0.000	1.212	1407	1394	1404	1416 s	1411 m	$\delta_{\text{NCH}}(30) + \nu_{\text{CC}}(25) + \delta_{\text{CCH}}(12)$
v_{58}	B_1	1419	1418	1398	37.064	0.424	1404	35.981	0.303	1408	1394	1404			$\delta_{\text{NCH}}(29) + \nu_{\text{CC}}(25) + \delta_{\text{CCH}}(12)$
v_{59}	A_1	1462	1468	1439	0.091	39.502	1454	0.079	48.158	1445	1463				$\Gamma_{\text{HCCH}}(34) + \delta_{\text{HCCH}}(30)$
v_{60}	B_2	1469	1474	1445	0.579	0.785	1459	0.691	0.410	1458	1452	1469	1441 w	1440 m	$\delta_{\text{HCH}}(31) + \Gamma_{\text{HCCH}}(27)$
v_{61}	A_1	1482	1487	1462	6.499	2.388	1477	2.987	2.656	1478	1465	1479			$\delta_{\text{HCH}}(30) + \Gamma_{\text{HCCH}}(30)$
v_{62}	B_2	1511	1511	1474	7.927	0.001	1483	6.748	0.044	1486	1465	1479	1475 vw		$\delta_{\text{CCH}}(37) + \delta_{\text{NCH}}(17) + \nu_{\text{CN}}(15)$
v_{63}	A_1	1512	1511	1475	1.997	7.686	1483	1.625	5.823	1486	1470	1489	1501 m	1509 vw	$\delta_{\text{CCH}}(37) + \delta_{\text{NCH}}(17) + \nu_{\text{CN}}(15)$
v_{64}	A_2	1595	1593	1548	0.000	5.495	1554	0.000	6.010	1558	1525	1536			$\nu_{\text{CC}}(45) + \nu_{\text{CN}}(30)$
v_{65}	B_1	1596	1593	1549	36.250	1.329	1555	34.686	1.646	1559	1526	1537	1557 m	1557 w	$\nu_{\text{CC}}(45) + \nu_{\text{CN}}(30)$
v_{66}	B_2	1633	1630	1583	122.192	8.921	1589	115.196	10.143	1593	1561	1572			$\nu_{\text{CC}}(60)$
v_{67}	A_1	1636	1632	1584	26.639	49.044	1591	24.717	54.552	1595	1562	1574	1605 vs	1606 m	$\nu_{\text{CC}}(60)$
v_{68}	A_1	2879	2879	2920	11.114	217.738	2917	16.254	175.776	2933	2931	2905 w	2902 m		$\nu_{\text{CH}_2}(100)$
v_{69}	B_2	2880	2882	2921	0.510	1.766	2917	0.697	1.727	2936	2934	2931	2929 w	2927 w	$\nu_{\text{CH}_2}(100)$
v_{70}	A_1	2888	2889	2933	61.686	12.142	2931	57.998	4.257	2946	2949	2947	2944 vs	2865 w	$\nu_{\text{CH}_2}(100)$
v_{71}	B_1	2900	2903	2946	3.138	118.881	2946	4.326	113.393	2957	2959	2971 vw	2975 vw	2933 w	$\nu_{\text{CH}_2}(100)$
v_{72}	A_2	2912	2912	2957	0.000	0.027	2955	0.000	0.028	2970	2968	2967			$\nu_{\text{CH}_2}(100)$
v_{73}	B_1	2933	2935	2978	44.513	8.188	2977	43.796	4.560	3000	2991	2992	2993 m	2992 vw	$\nu_{\text{CH}_2}(100)$
v_{74}	A_2	3011	3017	3038	0.000	208.827	3042	0.000	198.183	3050	3045	3051			$\nu_{\text{CH}}(90)$
v_{75}	B_1	3011	3017	3038	44.665	78.019	3042	43.103	77.038	3050	3045	3051	3025 m		$\nu_{\text{CH}}(90)$
v_{76}	B_2	3012	3018	3040	28.877	19.423	3043	37.108	15.544	3051	3047	3052	3029 m	3031 w	$\nu_{\text{CH}}(100)$
v_{77}	A_1	3012	3018	3040	8.960	134.921	3043	12.619	98.562	3051	3047	3052			$\nu_{\text{CH}}(99)$
v_{78}	A_2	3031	3034	3063	0.000	1.511	3064	0.000	0.219	3072	3071	3074			$\nu_{\text{CH}}(90)$
v_{79}	B_1	3031	3034	3063	72.525	7.170	3064	87.226	4.206	3072	3072	3074	3051 w	3056 vs	$\nu_{\text{CH}}(90)$
v_{80}	B_2	3034	3038	3065	0.006	20.105	3067	0.415	15.512	3075	3074	3077			$\nu_{\text{CH}}(99)$
v_{81}	A_1	3035	3038	3065	0.676	493.976	3067	0.184	470.874	3075	3074	3077	3073 vw		$\nu_{\text{CH}}(99)$
σ		29.63	28.61	14.68		14.65				17.80	16.94				

scis, scissoring; rock, rocking; twist, twisting; wag, wagging; asymm, asymmetric; symm, symmetric; str, stretching; tors, torsion; bend, bending; def, deformation; vs, very strong; s, strong; m, medium; w, weak; vw, very weak. IR: IR intensities (KM/mole); RA: Raman scattering activities (A**4/AMU).

^a Scaling factor: 0.9085.

^b Scaling factor: 0.8985.

^c Scaling factor: 0.9668.

^d Scaling factor: 0.9603.

^e Scaling factor: 0.9961.

^f Scaling factor: 0.9919.

^g Total energy distribution calculated B3LYP/6-311G(d,p) level.

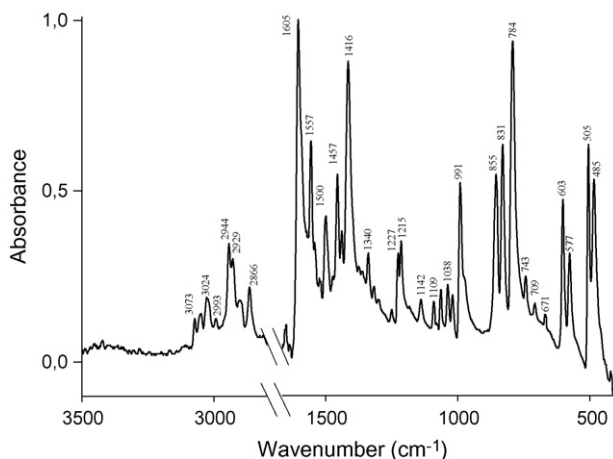


Fig. 4. The Infrared spectra of Bpp (in KBr).

vibrational analysis are given in the same tables. Vibrational assignments are based on the experimental information and the ab initio predicted frequencies of the molecule. To the best of our knowledge there is no vibrational data for gas phase Bpp molecule. Therefore we have to compare calculated results with those of solid phase (powder form) vibrational spectrum.

In the high frequency region ($3000\text{--}3500\text{ cm}^{-1}$), the C–H ring stretching modes are observed at $3073, 3051$ and 3024 cm^{-1} in the FT-IR spectrum and 3056 and 3031 cm^{-1} in the Raman spectrum, respectively. Eight C–H stretching modes ($\nu_{74}\text{--}\nu_{81}$) are predicted in the region from 3030 to 3070 cm^{-1} region. In this region, calculated B3LYP/6-31G (d) values are more reliable than other methods. As seen in Table 3, there is great mixing of the ring vibrational modes and also between the ring and subsistent modes. The descriptions of the modes are very complex because of the mixing different subsistent modes. Especially, the out of plane modes are the most difficult to be assigned due to mixing with the ring modes and also with the other

modes. Therefore, there are some strong frequencies useful to characterize in the IR and Raman spectra.

Ring breathing and raw methylene sensitive modes characterized at B3LYP/6-311G(d,p) level in Bpp molecule are plotted in Fig. 6. The vibrational motions are represented the vector corresponding to the atomic displacement for each atom and computed wavenumber. Displacements are indicated by dark arrow. Ring breathing and raw methylene sensitive modes appear characterized by direction of the displacement vector.

In the $2800\text{--}3000$ region, five CH_2 stretching modes ($\nu_{68}\text{--}\nu_{73}$) are also observed in the range from 2866 to 2992 cm^{-1} in the FT-IR spectrum and from 2859 to 2992 cm^{-1} in the Raman spectrum. The asymmetric vibration of the $-\text{CH}_2-$ group was observed at 2980 cm^{-1} for 1,2-bis(4-pyridyl)ethane (BPE) [6]. We observed at 2993 and 2917 cm^{-1} . The symmetric vibrations of the $-\text{CH}_2-$ group were observed also at 2870 cm^{-1} for BPE [6]. These modes observed at $2905, 2929$ and 2944 cm^{-1} . These vibrations are calculated at $2917\text{--}2931\text{ cm}^{-1}$ for symmetric vibrations and $2946\text{--}2977\text{ cm}^{-1}$ for asymmetric vibrations. Regarding the intensity, the calculated value of ν_s modes are slightly greater than the ν_{as} .

The experimental IR and Raman spectra of the title molecule shows absorption bands resulting from the skeletal vibrations of aromatic rings in the $1400\text{--}1600\text{ cm}^{-1}$ region. Ring CC and CN mode of pyridyl (mode ν_{67}) group is observed at 1605 cm^{-1} with the strongest absorption in the IR spectrum which is predicted at 1600 cm^{-1} ($\pm 5\text{ cm}^{-1}$) as a strong band. This mode however, is observed in the region between 1500 and 1560 cm^{-1} for metal square complexes of the Bpp ligand. CC and CN stretching modes of Bpp ligand reflect the perturbation caused by its coordination to the metal sites. Correa et al. [3] reported that this mode of pyridine rings, originally at 1602 and 1418 cm^{-1} in the free ligand, have been shifted to higher wavenumbers 1616 and 1429 cm^{-1} , respectively in the spectra of the complexes. With the metal coordination, CC and CN modes are not chang-

Table 4

Theoretically calculated optimized energy (a.u.), dipole moment (D), zero point vibrational energies (kcal/mol), rotational constants (GHz), entropies (cal/(mol K)) for Bpp (TT conformation)

	B3LYP		BLYP		HF	
	6-311G(d,p)	6-31G(d)	6-311G(d,p)	6-31G(d)	6-311G(d,p)	6-31G(d)
Optimized energy (a.u.)	-613.467461377	-613.318781814	-613.199104839	-613.038508514	-609.477458174	-609.344042896
Dipole Moment (Debye)	2.7156	2.7257	2.6507	2.6645	2.7952	2.8240
E_{HOMO} (eV)	-0.591	-0.277	-1.247	-0.916	-9.473	-9.377
E_{LUMO} (eV)	0.771	2.114	0.290	1.496	2.928	3.193
$\Delta E_{\text{H-L}}$ (eV)	1.362	2.391	1.537	2.412	12.401	12.570
Zero point energy (kcal/mol)	152.15530	153.27928	147.53688	148.53833	162.53725	164.16821
Rotational constants (GHz)						
A	1.67067	1.65901	1.65344	1.63809	1.69935	1.69240
B	0.20489	0.20470	0.20120	0.20121	0.20660	0.20671
C	0.20176	0.20165	0.19803	0.19817	0.20345	0.30362
Entropy (cal/(mol K))						
Total	120.047	119.345	122.904	120.805	114.458	114.493
Translational	41.756	41.756	41.756	41.756	41.458	41.756
Rotational	31.432	31.440	31.479	31.487	31.398	31.401
Vibrational	46.860	46.149	49.669	47.562	41.304	41.336

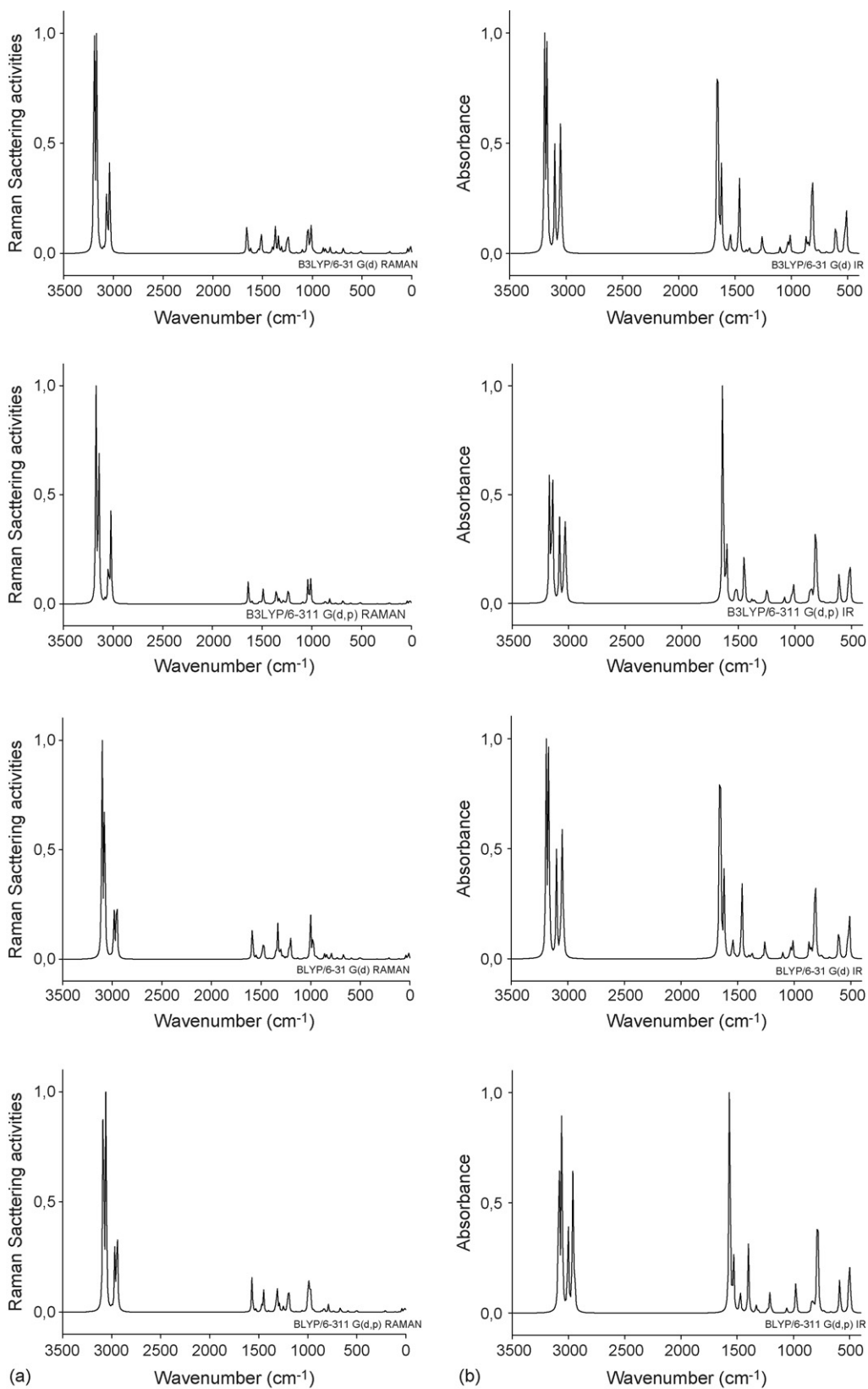


Fig. 5. Theoretical computed Raman (a) and IR (b) spectra of Bpp.

ing significantly. As seen in Table 3, theoretically, two bands were calculated close to each other and scaled at 1589 cm^{-1} (B_2 symmetry) and 1595 cm^{-1} (A_1 symmetry) for B3LYP/6-31G(d) level. Both modes appear strongly coupled but the first band is calculated with higher intensity. As we know from experimental IR and Raman spectra, only one band was detected at 1605 and 1606 cm^{-1} , respectively.

The band at 1557 cm^{-1} (IR) is medium and should include also the CC and CN stretching vibration, which for 1,2-bis(4-pyridyl)ethane [6] and *trans*-1,2-bis(4-pyridyl)ethylene [15] are located at 1558 (IR)– 1559 (Ra), 1550 cm^{-1} (IR, Ra), respectively. The corresponding band appearing at the calculated frequencies of 1554 and 1555 cm^{-1} (mw) are coupled to the pyridyl ring CC and CN and in plane C–H bending vibration. These assignments are support by the TED values. The modes

ν_{62} and ν_{63} are attributed to the ip C–H bending vibration and are observed in FT-Raman 1509 (vw), in FT-IR 1475 (vw)– 1500 (vw) cm^{-1} . The modes ν_{60} is attributed to CH₂ scissors vibration and is observed in FT-Raman 1440 (m) and in FT-IR 1441 (w). Similar comparative analysis has been made for the other selected strong or medium bands.

4.3. Other molecular properties

Several calculated thermodynamic parameters are presented in Table 4. Total energies are found to decrease with the increase of the basis set dimension. The changes in total entropy of Bpp at room temperature at different basis set are only marginal.

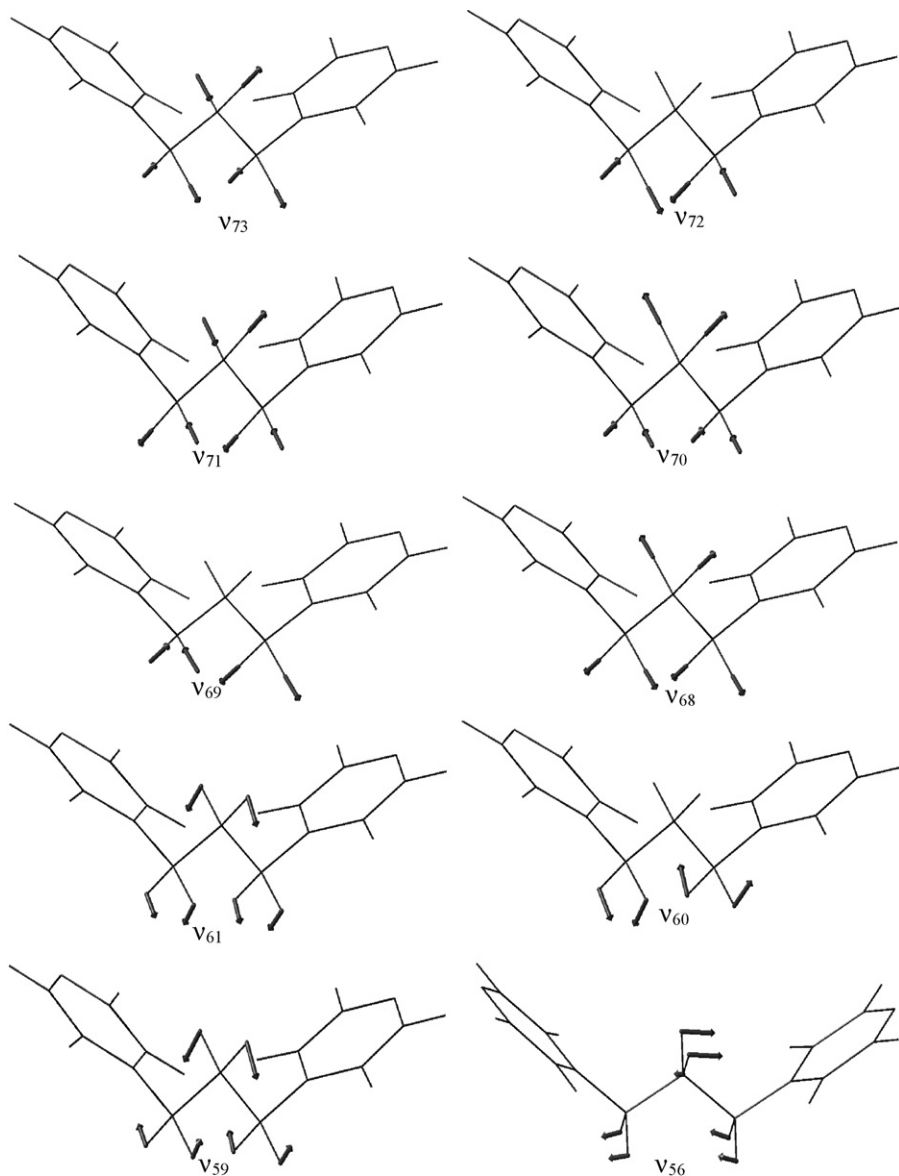


Fig. 6. Some raw modes of methylene group and ring breathing for B3LYP/6-311G(d,p).

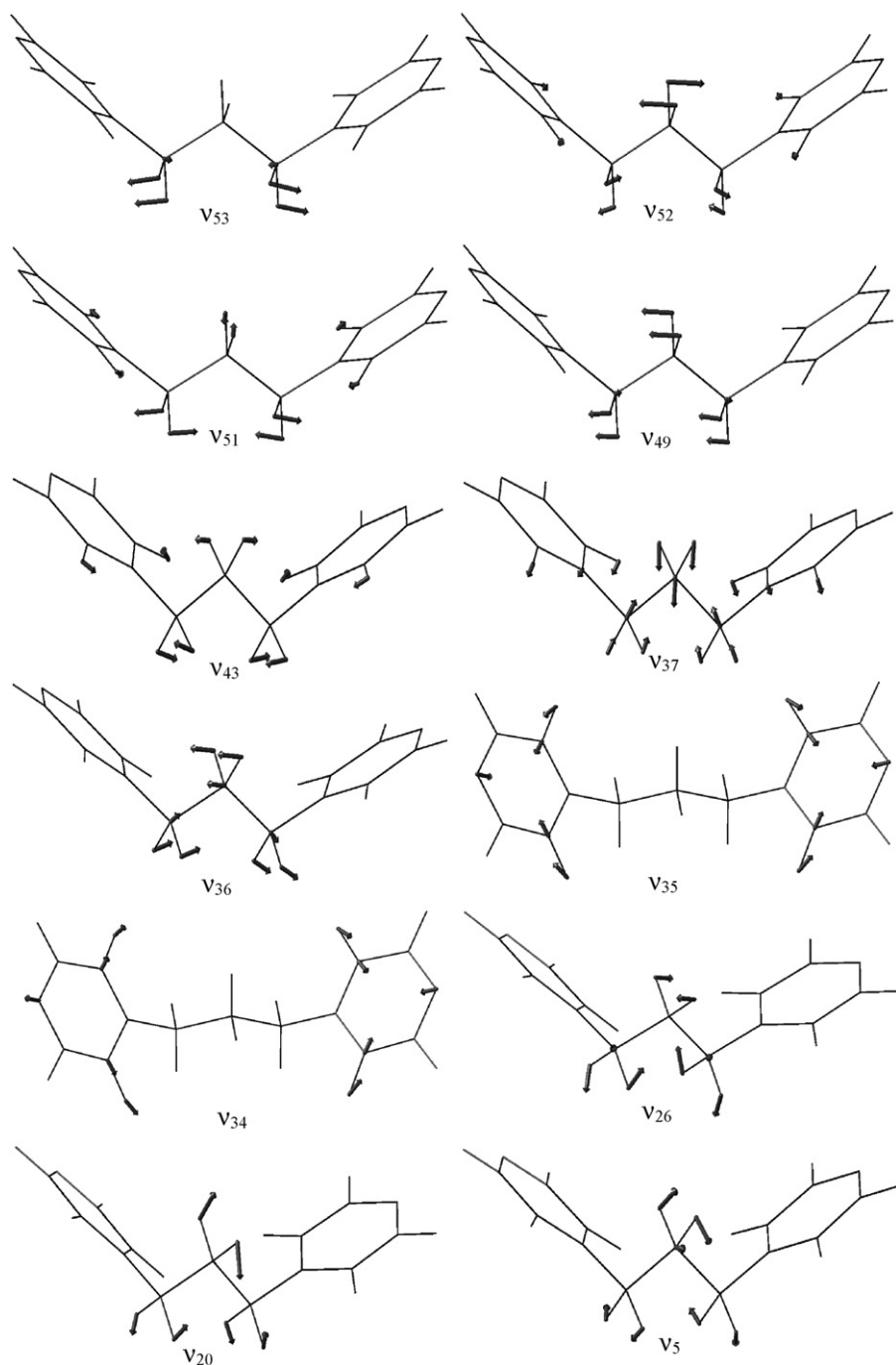


Fig. 6. (Continued).

5. Conclusion

We have carried out DFT and ab initio calculations on the structure and vibrational spectrum of Bpp. Comparison between the calculated and experimental structural parameters indicates that B3LYP results are in good agreement with experimental ones. On account of the fact that Bpp has examined and reassessments of some vibrational modes are proposed. The good agreement between the frequencies calculated by B3LYP/6-31G(d), and experimental results indicates that the density functional methods are reliable and provides val-

able information for understanding the vibrational spectra of molecule.

References

- [1] T.W. Lee, J.P.K. Lau, W.T. Wong, Polyhedron 23 (2004) 999.
- [2] M.J. Plater, M.R. St.J. Foreman, T. Gelbrich, S.J. Coles, M.B. Hursthouse, J. Chem. Soc., Dalton Trans. 18 (2000) 3065–3073.
- [3] C.C. Correa, R. Diniz, L.H. Chagas, B.L. Rodrigues, M.I. Yoshida, W.M. Teles, F.C. Machado, L.F.C. Oliveira, Polyhedron 26 (2007) 989–995.
- [4] E.Q. Gao, Y.X. Xu, A.L. Cheng, M.Y. He, C.H. Yan, Inorg. Chem. Commun. 9 (2006) 212–215.

- [5] Y. Kim, S.J. Kim, S.H. Choi, J.H. Han, S.H. Nam, J.H. Lee, H.J. Kim, C. Kim, D.W. Kim, H.G. Jang, Inorg. Chim. Acta 359 (2006) 2534–2542.
- [6] M. Kurt, Ş. Yurdakul, J. Mol. Struct. 654 (2003) 1–9.
- [7] S.H. Vosko, L. Wilk, M. Nusair, Can. J. Phys. 58 (1980) 1200.
- [8] <http://srdata.nist.gov/cccdb/vsf.asp>.
- [9] M.J. Frisch, G.W. Trucks, H.B. Schlegel, G.E. Scuseria, M.A. Robb, J.R. Cheeseman, J.A. Montgomery Jr., T. Vreven, K.N. Kudin, J.C. Burant, J.M. Millam, S.S. Iyengar, J. Tomasi, V. Barone, B. Mennucci, M. Cossi, G. Scalmani, N. Rega, G.A. Petersson, H. Nakatsuji, M. Hada, M. Ehara, K. Toyota, R. Fukuda, J. Hasegawa, M. Ishida, T. Nakajima, Y. Honda, O. Kitao, H. Nakai, M. Klene, X. Li, J.E. Knox, H.P. Hratchian, J.B. Cross, C. Adamo, J. Jaramillo, R. Gomperts, R.E. Stratmann, O. Yazyev, A.J. Austin, R. Cammi, C. Pomelli, J.W. Ochterski, P.Y. Ayala, K. Morokuma, G.A. Voth, P. Salvador, J.J. Dannenberg, V.G. Zakrzewski, S. Dapprich, A.D. Daniels, M.C. Strain, O. Farkas, D.K. Malick, A.D. Rabuck, K. Raghavachari, J.B. Foresman, J.V. Ortiz, Q. Cui, A.G. Baboul, S. Clifford, J. Cioslowski, B.B. Stefanov, G. Liu, A. Liashenko, P. Piskorz, I. Komaromi, R.L. Martin, D.J. Fox, T. Keith, M.A. Al-Laham, C.Y. Peng, A. Nanayakkara, M. Chalacombe, P.M.W. Gill, B. Johnson, W. Chen, M.W. Wong, C. Gonzalez, J.A. Pople, Gaussian 03 Revision C.02, Gaussian, Inc., Wallingford, CT, 2004.
- [10] A. Firsch, A.B. Nielsen, A.L. Holder, Gaussview Users Manual, Gaussian Inc., Pittsburgh, PA, 2000.
- [11] L. Carlucci, G. Ciani, D.M. Proserpio, S. Rizzato, Cryst. Eng. Commun. 4 (22) (2002) 119–121.
- [12] M.C. Suen, H.A. Tsai, J.C. Wang, J. Chin. Chem. Soc. (2006) 305–312.
- [13] S.J. Hong, H. Kwak, Y.M. Lee, C. Kim, Y. Kim, S.J. Kim, Anal. Sci. X-ray Struct. Anal. Online 21 (2005) 203–204.
- [14] P. Pulay, J. Baker, K. Wolinski, 2013 Green Acres Road, Suite A, Fayetteville, AR 72703, USA.
- [15] Z. Zhuang, J. Cheng, H. Jia, J. Zeng, X. Han, B. Zhao, H. Zhang, W. Zhao, Vibr. Spectrosc. 43 (2007) 306–312.